

Supporting Information

Sensitive Label-Free Monitoring of Protein Kinase Activity and Inhibition Using Ferric Ions Coordinating to Phosphorylated Sites As Electrocatalysts

Min Wang, Gui-Xia Wang, Fang-Nan Xiao, Yun Zhao, Kang Wang, and Xing-Hua Xia*

Table of Contents

1. Experimental Section
2. Electrochemical impedance measurements
3. Characterization of the P-peptide and peptide modified electrode
4. Study of the peaks for the Fe(III)-P-peptide modified electrode
5. UV-vis Characterization of Fe(III) and P-peptide
6. Electrochemical detection of hydrogen peroxide
7. Quantitative Detection of PKA by DPV
8. Feasibility validation for acidic substrate peptides

Supporting information

1. Experimental Section

Reagents

The substrate peptide (LRRASLGGGGC) was synthesized by Sangon Biotech Co., Ltd. (Shanghai, China). LRRASLGDDDC was synthesized by Shanghai science peptide Biological Technology Co., Ltd. Protein Kinase A (PKA, Catalytic subunit from bovine heart), Adenosine triphosphate (ATP), DL-Dithiothreitol (DTT), 1-hexanethiol (HT), PKA inhibitor H-89 dihydrochloride hydrate and N-Ethyl-N-(3-dimethyl-aminopropyl) carbodiimide hydrochloride (EDC) were purchased from Sigma-Aldrich. Quality-controlled serum was purchased from BioSino Bio-technology and Science Inc. (Beijing, China). All other reagents were of analytical grade. All solutions were prepared using ultrapure water (18.3 MΩ·cm) from the Millipore Milli-Q system.

Preparation of peptide-SAM modified gold electrodes

Gold electrode (2 mm in diameter, CH Instruments Inc.) was first polished with 0.05 μm alumina slurry, followed by sonication in ethanol and water each for 5 min, respectively. Then the electrode was cleaned in 0.5 M H₂SO₄ by running a cyclic voltammetry (CV) cycle between 0 and 1.5 V until a stable cyclic voltammogram of the typical polycrystalline electrode was obtained. Preparation of the porous gold electrode: The clean electrode was first anodized at 5 V in 0.1 M phosphate buffer solution (pH 7.4) for 5 min to form oxidized gold surface. Then, the gold oxides were chemically reduced in a 1.0 M β-D-glucose aqueous solution at 4 °C for 5 min and cleaned by water. After being dried with nitrogen, the cleaned gold working electrode was immediately coated with 4 μL of 0.2 mM peptide solution and kept at 4 °C for 16 h to allow the self-assembly of peptide on the gold electrode. Afterward, the electrode was thoroughly rinsed with blank Tris-HCl buffer solution (10 mM, pH 7.5, 25 °C, TBS). The peptide-modified gold electrode was then immersed in 0.1 mM HT ethanol solution for 30 min to block the unmodified region of the electrode, followed by rinsing with blank TBS.

Peptide phosphorylation on modified gold electrodes

Protein kinase A was first dissolved in Tris-HCl buffer (20 mM, pH 7.5, 25 °C) containing 50 mM NaCl, 1 mM EDTA, 2 mM 1,4-Dithiothreitol (DTT) and 50% glycerol. PKA reaction mixture contained a desired concentration of PKA, 0.2 mM ATP and 10 mM MgCl₂ in 80 μL Tris-HCl buffer (20 mM, pH 7.5, 25 °C). In a typical phosphorylation experiment, the peptide-modified gold electrode was incubated in the above reaction mixture at 30 °C for 2 h. For the inhibition experiments, different concentration of PKA inhibitor H-89 was included in the reaction mixture. After 4 h of incubation at 30 °C, the inhibition reaction was terminated and then the electrode was rinsed using blank TBS. In addition, serum samples were prepared by adding a desired concentration of PKA in serum instead of Tris-HCl buffer. The peptide-modified gold electrode was then incubated in serum samples at 30 °C for 2 h.

Immobilization of iron(III) ion on phosphorylation sites.

The as-prepared phosphorylated peptide electrode was immersed in a FeCl₃ solution (50 mM, containing 100 mM HCl, pH 1.0) for 1 h at room temperature. After the electrodes were carefully washed with 100 mM HCl and water, respectively, electrochemical measurements were carried out.

In order to validate the feasibility for acidic substrate peptides, a cleaned gold electrode was coated by 4 μL of 0.2 mM peptide solution (LRRASLGDDDC). Then, the peptide modified electrode was immersed in 0.1 M HEPES (pH 7.4) containing 0.1 M EDC and 0.01 M butylamine for 2 h to block the carboxyl residues, followed by immersing in 0.1 mM HT for 30 min. Other procedures are the same as those mentioned in our experimental section.

Instruments

Electrochemical impedance spectroscopy (EIS) measurements were carried out with an Ivium Compact Stat.e (Ivium, The Netherlands). Other electrochemical measurements were carried out on a CHI 660D electrochemical working station (CH Instruments, USA) using a three-electrode system with a modified gold electrode (2 mm in diameter) as the working electrode. A platinum wire and an Ag/AgCl reference electrode (saturated KCl) were used as the counter and reference electrodes, respectively. The scan rate used in cyclic voltammetry (CV) was 0.2 V/s without special demonstration. The data of differential pulse voltammetry (DPV) were obtained with a potential step of 5 mV, pulse amplitude of 50 mV, pulse width of 50

ms and apulse period of 100 ms. The error bars represent relative standard deviations for three independent measurements. UV-vis absorption spectra were performed on a UV 3600 spectrophotometer (Shimazu, Japan).

2. Electrochemical impedance measurements

Electrochemical impedance spectroscopy (EIS) was used to monitor the modification process of the electrode. As shown in Figure S1 and Table S1, the R_{et} values of peptide modified electrode and peptide modified electrode blocked by HT are much larger than that of the bare gold electrode, since the immobilized peptide and HT can hinder the electron transfer of the redox probes $Fe(CN)_6^{3-/4-}$. After phosphorylation of peptide, the added negative charge from phosphate groups repel $Fe(CN)_6^{3-/4-}$ and thus further increase the R_{et} of P-peptide modified electrode. The immobilized Fe^{3+} on phosphorylated sites by coordinate bonds will neutralize partial negative charge, which decreases the repelling force between $Fe(CN)_6^{3-/4-}$ and the electrode and thus decreases the R_{et} of Fe(III)-P-peptide modified electrode. These results demonstrate that the modification process of the electrode has been achieved successfully.

3. Characterization of the P-peptide and peptide modified electrode

The CV of the P-peptide modified electrode (Figure S2, curve d) shows a pair of quasi-reversible current peaks ($E_{pa}= 0.353$ V, $E_{pc}= 0.178$ V). The pair of peaks is not caused by electron transfer between the assembled species and the electrode since all of the immobilized species on modified electrode are nonelectroactive. Similar to the P-peptide modified electrode, the CV of the electrode assembled with peptide blocked by HT shows a pair of current peaks (Figure S2, curve c). To investigate the origin of the current peaks, the CVs of the electrodes assembled with HT and peptide are compared (Figure S2, curves a-b). No obvious current peaks are observed at the HT modified electrode. However, a pair of reversible current peaks located at 0.299 V and 0.382 V appears clearly for the peptide modified electrode, which implies that the current peaks of the P-peptide modified electrode origins from the peptide. According to the reported results¹⁻² and the structure of substrate peptide (Figure S3), it is reasonable to assign the current peaks of peptide modified electrode to the electric field driven protonation/deprotonation of amino groups and carboxyl groups in peptide residues.

It is well-known that the electric field driven protonation/deprotonation is dominated by a surface controlled process and both the peak current and the half-wave potential ($E_{1/2}$) are functions of solution pH. Therefore, the influence of scan rate and buffer pH on the current peaks was investigated in depth. As shown in Figure S4A, the peak current increases linearly with scan rate between 0.01 V/s and 1 V/s, suggesting a surface controlled process. The significant change of these peaks is observed with the varying pH (Figure S4B). The cathodic peak potential of current peaks shifts cathodically with increasing pH at a rate of 24 mV/pH (Figure S4C) and both anodic and cathodic peak currents decrease as the solution pH increases (Figure S4D). The above results confirm that the observed peaks for peptide modified electrode should be attributed to the protonation/deprotonation. However, the dependence of peak current and formal potential on solution pH for peptide modified electrode are more complicated than that for electrodes assembled with simplex end-group species since both the amino groups and carboxyl groups in the substrate peptide can be protonated and deprotonated.

4. Study of the peaks for the Fe(III)-P-peptide modified electrode

For the Laviron's equation, I_p is the anodic peak current, n is the number of electrons (assuming $n = 1$), A is the effective area of the gold electrode (0.0708 cm^2 , which is determined by the integration of the cathodic peak at ca. 0.9 V from the CV in 0.5 M H_2SO_4) and v is the scan rate.

The formal potential of Fe(III)/Fe(II) redox couple is different from that of free $\text{Fe}^{3+}/\text{Fe}^{2+}$ in aqueous and other electroactive species containing Fe(III)/Fe(II) redox couple (such as heme in cyt c, a detailed comparison is shown in Table S2). This result could be explained by the difference in chemical environment (different ligands and coordination number). In order to understand the environmental difference in depth, CVs of the Fe(III)-P-peptide modified electrode in 5 mM HEPES (250 mM KCl, pH 1.5) in the absence and presence of 5 mM FeCl_3 were performed (Figure S6, curves b-c). With the addition of FeCl_3 , an additional pair of redox peaks appears at 0.494 V. Their peak currents increase upon successive addition of FeCl_3 (Figure S7A) and the formal potential is consistent with that for a bare gold electrode (Figure S7B), which implies that the additional redox peaks are assigned to free $\text{Fe}^{3+}/\text{Fe}^{2+}$ in aqueous indeed. As shown in Figures S7C and S7D, the scan rate dependence of the additional peaks shows that the peak current increases linearly with the square root of

scan rate, corresponding to a diffusion controlled process. (Note: in order to more clearly investigate the pH influence and the environmental difference, the porous gold electrodes are used in these sections).

5. UV-vis Characterization of Fe(III) and P-peptide

It is well-known that ferric ions can coordinate with phosphate groups with high affinity and specificity. To demonstrate the existence of the coordination interaction between ferric ions and phosphate groups, UV-vis absorption spectra of the P-peptide with ferric ions were recorded. In order to phosphorylate the peptides, PKA was introduced into the peptide solution and the resultant mixture was kept at 30 °C for 2 h. The contained PKA is not removed after the phosphorylation of peptide. As shown in Figure S8, UV-vis absorption between 200 nm and 450 nm is associated to the free ferric ions and the absorption at 258 nm is assigned to the unremoved PKA. In the presence of the P-peptide, the absorption peak of ferric ions shifts to the lower wavelength (below 400 nm). This result demonstrates that ferric ions can interact with phosphate groups of P-peptide, which results in the change of the chemical environment of ferric ions and further the change of the electronic energy state.

6. Electrochemical detection of hydrogen peroxide

Based on the electrocatalytic property of Fe(III)-P-peptide modified electrode, a simple electrochemical sensor for H₂O₂ was developed. The performance of this sensor was tested by recording the amperometric responses upon successive addition of H₂O₂. Figure S10A shows that the cathodic current at the Fe(III)-P-peptide modified electrode increases with the injected H₂O₂. The calibrated steady-current responses with H₂O₂ concentration are given in Figure S10B. The relationship is linear up to 10 mM with a detection limit of 2.7 μM, which is comparable with previous reports.³⁻⁴

7. Quantitative Detection of PKA by DPV

Monitoring the voltammetric response of the immobilized electroactive ferric ions provides a label-free approach for the detection of PKA. DPV was used for measuring the electrochemical response for the reduction of ferric ions. As shown in Figure S11, the corresponding current increases with the concentration of PKA and reaches the

saturation condition when the PKA concentration is higher than 50 U/mL. The dependence of the peak current on PKA concentration is depicted in Figure S10B. The relationship is approximately linear up to 25 U/mL. This method enables the analysis of PKA with a minimum detectable concentration of 3 U/mL, which is the average level for the detection of protein kinases according to previous reports⁵⁻⁶.

8. Feasibility validation for acidic substrate peptides

Ferric ions show good affinity to phosphate groups and carboxyl residues by coordination interaction. However, the interference induced by the carboxyl groups will reduce the signal-to-noise ratio and thus the sensitivity of the as-proposed strategy. For the model substrate peptide (LRRASLGGGGC), only one carboxyl group is contained, which hardly influences the sensitivity of our strategy. However, for the acidic peptides, it is necessary to block the carboxyl groups using a blocking agent for the lower background response and the higher sensitivity. In order to validate the feasibility for acidic substrate peptides, LRRASLGDDDC (containing four carboxyl groups) was used as a model acidic substrate for PKA. Butylamine was used as a model agent to block the carboxyl groups via amidation reaction in the presence of EDC.

As shown in Figure S12, a decrease in both the background and signal responses was observed after the blockage of carboxyl residues. However, the decrease in the absence of PKA is larger than that in the presence of PKA, which suggests an increased signal-to-noise ratio effectively after the blockage of carboxyl residues with butylamine (Table S4). These results demonstrate that the as-proposed strategy shows potential applications in various kinase activity analysis, even with the acidic substrate peptides.

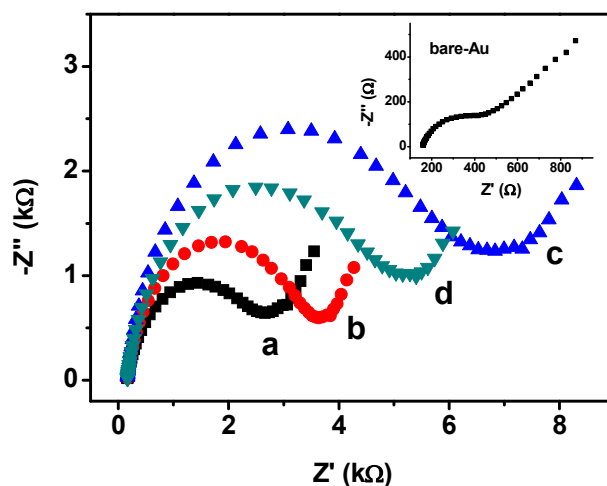


Figure S1. Nyquist plots of the different modified electrodes in 5 mM Fe(CN)₆^{3-/4-} solution containing 0.1 M KCl): (a) peptide modified electrode; (b) peptide modified electrode blocked by HT; (c) P-peptide modified electrode; (d) Fe(III)-P-peptide modified electrode. Inset: The Nyquist plot of a bare gold electrode. These measurements were carried out under open-circuit conditions. The AC voltage amplitude was 7 mV and the frequencies ranged from 10⁵ Hz to 1 Hz.

Table S1. The electron transfer resistance of the modified gold electrodes.

	bare Au	peptide-Au	peptide/HT-Au	P-peptide/HT-Au	Fe(III)-P-peptide/HT-Au
R_{et} /ohm	301	2429	3243	6340	4779

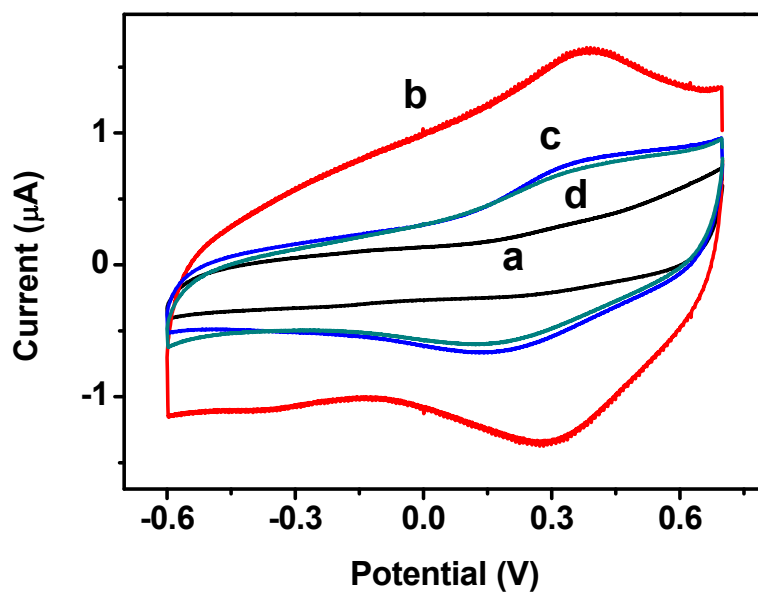


Figure S2 CVs of the gold electrodes assembled with HT (a), peptide (b), peptide blocked by HT (c) and phosphorylated peptide (d, PKA concentration: 50 U/mL) in 5 mM PBS (250 mM KCl, pH 7.00).

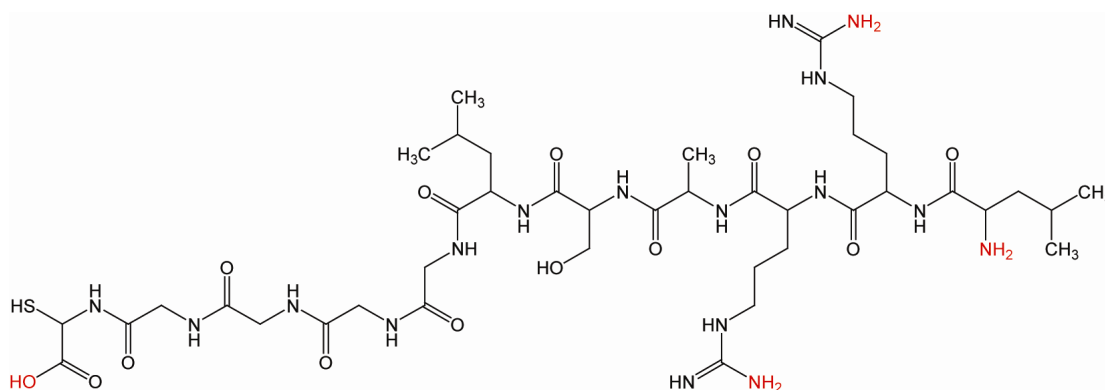


Figure S3. The structure of substrate peptide (LRRASLGGGGC).

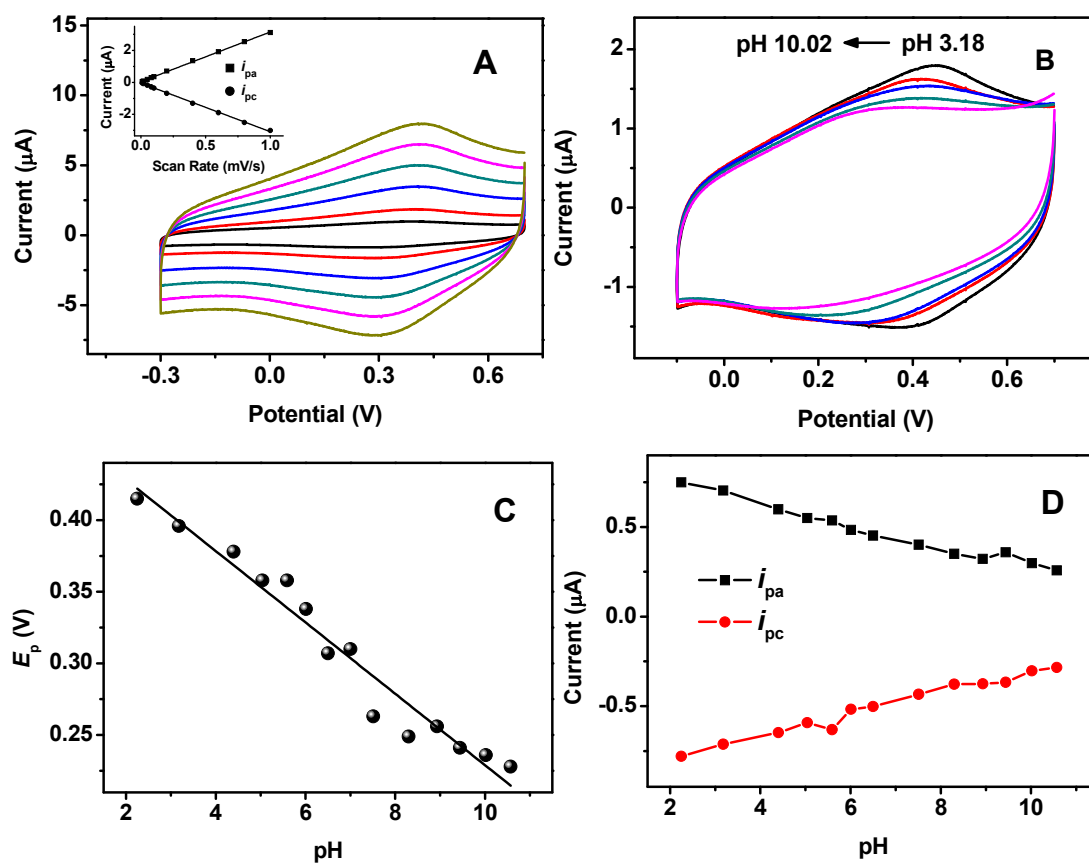


Figure S4 (A) CVs of the peptide modified gold electrode in 5 mM PBS (250 mM KCl, pH 7.00) at 0.1, 0.2, 0.4, 0.6, 0.8 and 1 V/s (from internal to external). Inset: Plots of anodic and cathodic peak currents versus scan rate. (B) pH-dependent CVs of the peptide modified gold electrode. (C) Plot of the cathodic peak potential versus pH (from external to internal: 3.18, 5.04, 6.50, 8.30, 10.02). (D) Plots of the maximum anodic and cathodic peak currents versus pH.

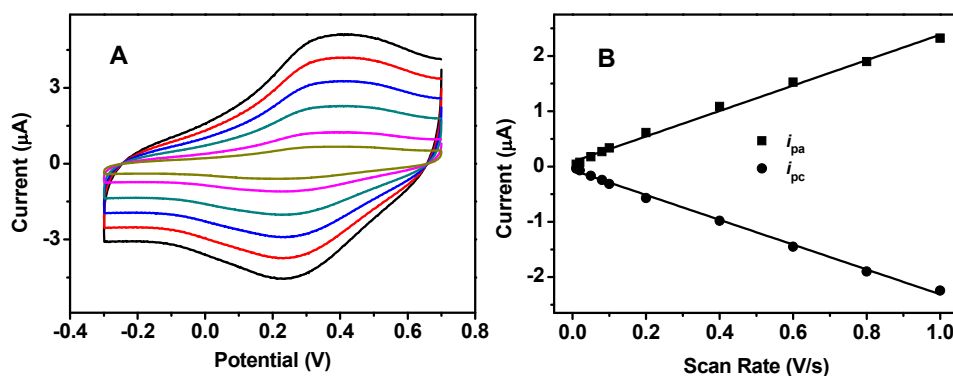


Figure S5 (A) CVs of the Fe(III)-P-peptide modified gold electrode in 5 mM PBS (250 mM KCl, pH 7.00) at 0.1, 0.2, 0.4, 0.6, 0.8 and 1 V/s (from internal to external). (B) Plots of anodic and cathodic peak currents versus scan rate for the Fe(III)-P-peptide modified gold electrode.

Table S2 Comparison of different species containing Fe(III)/Fe(II) redox couple.

Types	E° / V (vs. Ag/AgCl)
Fe ³⁺ /Fe ²⁺	0.574
Fe(CN) ₆ ^{3-/4-}	0.353
HRP (heme)	-0.26 ⁷
Cyt c (heme)	0.024 ⁸
Fe(III)-P-peptide	0.316

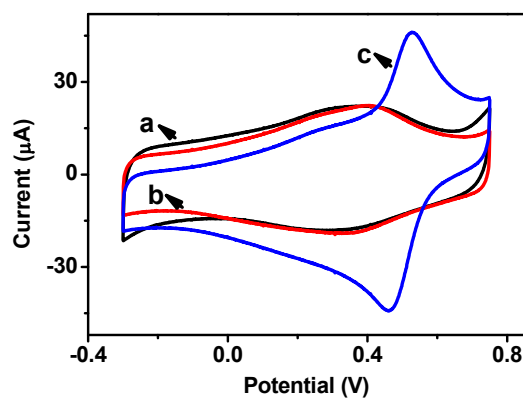


Figure S6 CVs of the Fe(III)-P-peptide modified porous gold electrode in 5 mM HEPES (250 mM KCl, pH 7.0) (a) and 5 mM HEPES (250 mM KCl, pH 1.5) without (b) and with 5 mM FeCl₃ (c). PKA concentration is 50 U/mL.

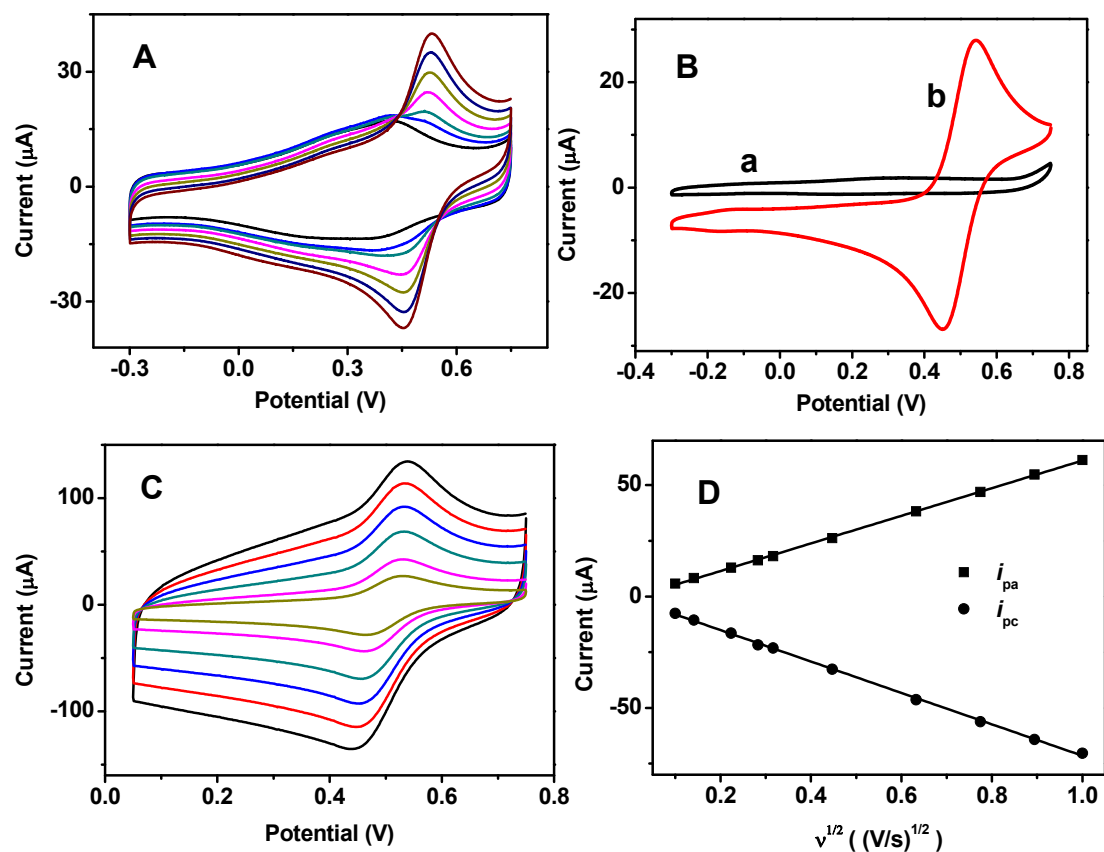


Figure S7 (A) CVs of the Fe(III)-P-peptide modified electrode in 5 mM HEPES (250 mM KCl, pH 1.5) containing 0, 0.5, 1, 2, 3, 4 and 5 mM FeCl_3 . (B) CVs of the bare gold electrode in 5 mM HEPES (250 mM KCl, pH 1.5) without (a) and with (b) 5 mM FeCl_3 . (C) CVs of the Fe(III)-P-peptide modified gold electrode in 5 mM HEPES (250 mM KCl, pH 7.00) containing 5 mM FeCl_3 at 0.1, 0.2, 0.4, 0.6, 0.8 and 1 V/s (from internal to external). (D) Plots of anodic and cathodic peak currents versus the square root of scan rate. Note: In this section, HEPES buffer was used instead of PBS buffer since the free ferric ions is not stable in PBS buffer.

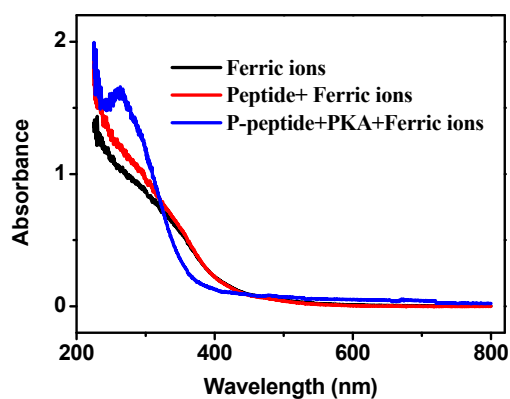


Figure S8 UV-vis absorption spectra of ferric ions, ferric ions in the presence of the peptide and P-peptide (containing PKA).

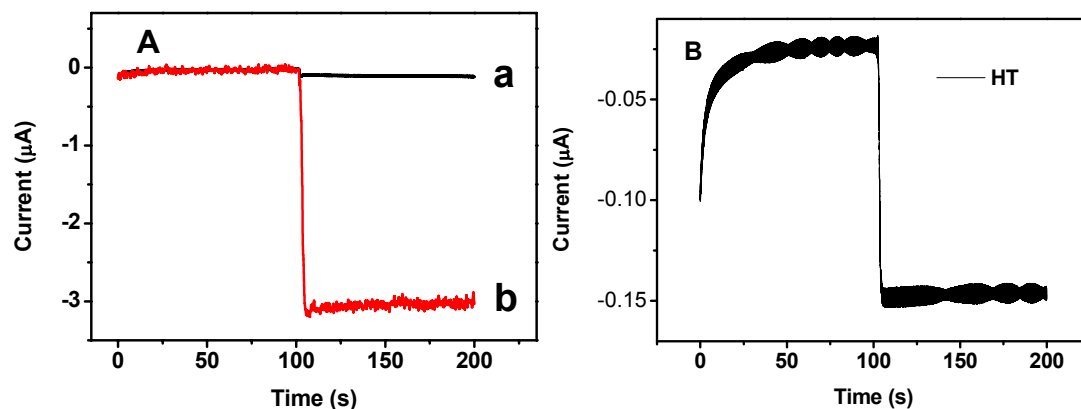


Figure S9 (A) Amperometric responses of the gold electrodes assembling P-peptide without (a) and with (b) coordinating Fe³⁺ at -0.4 V in 5 mM PBS (250 mM KCl, pH 7.00) upon the addition of 1 mM H₂O₂. (B) Amperometric responses of the gold electrodes assembling with HT instead of peptide at -0.4 V in 5 mM PBS (250 mM KCl, pH 7.00) upon the addition of 1 mM H₂O₂.

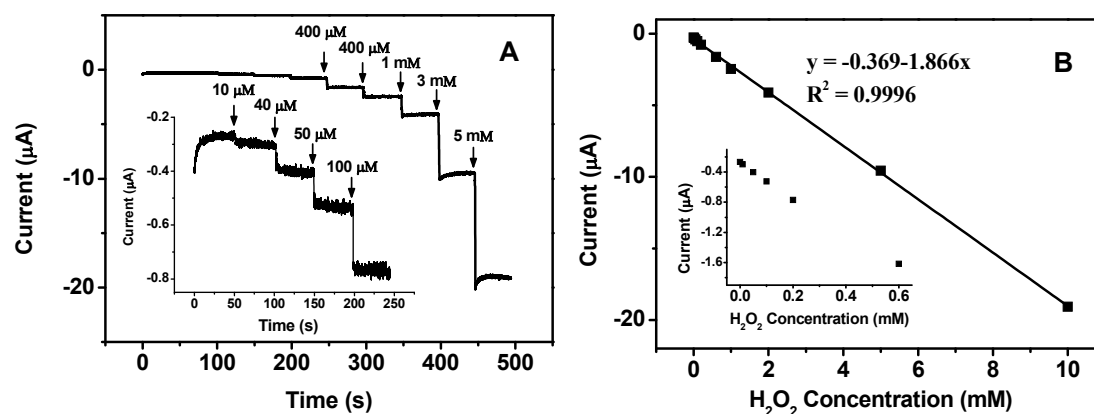


Figure S10 (A) Amperometric responses of the Fe(III)-P-peptide modified gold electrode at -0.4 V in 5 mM PBS (250 mM KCl, pH 7.00) upon successive addition of H₂O₂. (B) Plots of electrocatalytic current versus H₂O₂ concentration between 10 µM and 10 mM.

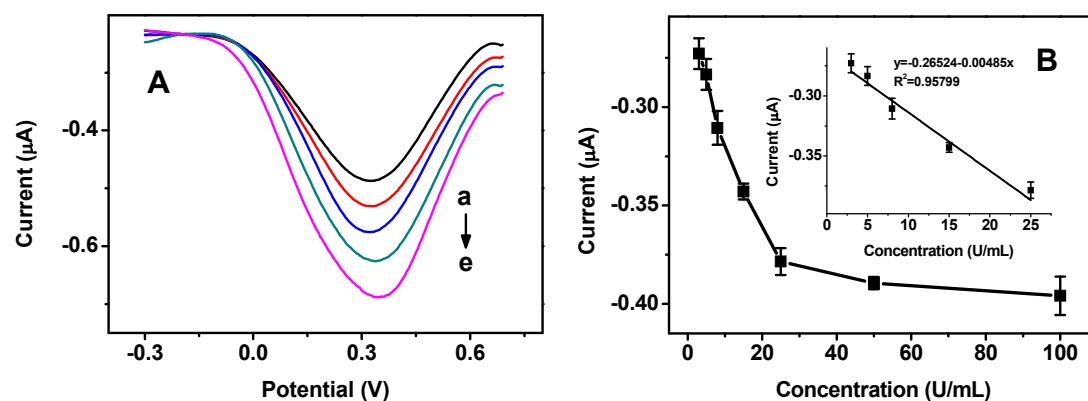


Figure S11 (A) DPVs of Fe(III)-P-peptide modified electrodes for kinase activity assays in the presence of (a-e) 0, 3, 5, 15 and 50 U/mL PKA. (B) Plots for the dependence of peak current on the concentration of PKA. Inset: Plot of peak current on the concentration of PKA between 3 and 25 U/mL.

Table S3 Detection of PKA in serum with the as-proposed strategy.

Sample Numbers	Standard PKA concentration (U/mL)	PKA concentration detected by the as-proposed strategy (U/mL)	Relative error (%)
1	5	5.41	8.20
2	8	6.94	13.25

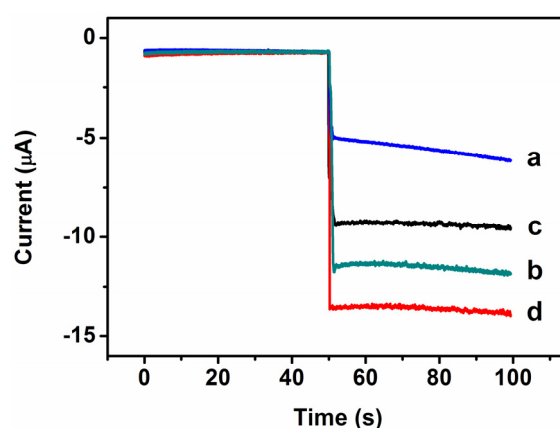


Figure S12 Amperometric responses of the Fe(III)-P-peptide modified gold electrodes for kinase activity with (curves a and b) and without (curves c and d) the blockage carboxyl residues in the presence of 0 (curves a and c) and 50 U/mL PKA (curves b and d) at -0.4 V upon the addition of 10 mM H₂O₂.

Table S4 Electrocatalytic responses of H₂O₂ in different conditions.

	No blockage	Blockage	Decreased Values/ µA
In the absence of PKA/ µA	8.557	4.440	4.117
In the presence of PKA/ µA	12.793	10.636	2.157

References

1. I. Burgess, B. Seivewright and R. B. Lennox, *Langmuir*, 2006, **22**, 4420-4428.
2. M. Wang, F. N. Xiao, K. Wang, F. B. Wang and X. H. Xia, *J. Electroanal. Chem.*, 2013, **688**, 304-307.
3. J. D. Qiu, H. Z. Peng, R. P. Liang, J. Li and X. H. Xia, *Langmuir*, 2007, **23**, 2133-2137.
4. Y. Chen, F. B. Wang, L. R. Guo, L. M. Zheng and X. H. Xia, *J. Phys. Chem. C*, 2009, **113**, 3746-3750.
5. J. Ji, H. Yang, Y. Liu, H. Chen, J. Kong and B. Liu, *Chem. Commun.*, 2009, 1508-1510.
6. K. Kerman, M. Chikae, S. Yamamura and E. Tamiya, *Anal. Chim. Acta*, 2007, **588**, 26-33.

7. Q. Zhang, Y. Qiao, F. Hao, L. Zhang, S. Y. Wu, Y. Li, J. H. Li and X. M. Song, *Chem. Eur. J.*, 2010, **16**, 8133-8139.
8. X. Chen, H. Y. Long, W. L. Wu and Z. S. Yang, *Thin Solid Films*, 2009, **517**, 2787-2791.